Exchange interaction through amorphous intergranular layers in a two-phase system

2000 J. Phys.: Condens. Matter 12 3255

(http://iopscience.iop.org/0953-8984/12/14/304)

J. Phys.: Condens. Matter **12** (2000) 3255–3265. Printed in the UK PII: S0953-8984(00)06415-8

Exchange interaction through amorphous intergranular layers in a two-phase system

J Arcas†, A Hernando†, C Gómez-Polo‡, F J Castaño†, M Vázquez†, A Neuweiler§ and H Krönmuller§

† Instituto de Magnetismo Aplicado (UCM, RENFE), PO Box 155, 28230, Las Rozas, Madrid, Spain

‡ Departamento de Física, Universidad Pública de Navarra, 31006 Pamplona, Spain

§ Max Planck Institut für Metallforschung, Heisenbergstraße 1, D-70569 Stuttgart, Germany

Received 28 July 1999, in final form 24 January 2000

Abstract. Amorphous melt spun ribbons of composition $Fe_{87.2}Zr_{7.4}B_{4.3}Cu_{1.1}$ have been annealed at temperatures between 713 K and 923 K, achieving different stages of the nanocrystallization process. The sample annealed at 748 K shows a large magnetic hardening at room temperature as well as an irregular domain pattern. Both are attributed to the presence of non-coupled crystallites. When cooled to 250 K, the coercivity of this sample decreases steeply as the crystallites become coupled. The samples as cast and annealed at higher temperatures are magnetically soft and show wide regular domains. The above mentioned results as well as the thermal dependence of the coercivity are qualitatively described in the framework of a previously proposed model that accounts for the effective anisotropy in two-phase nanocrystalline materials.

1. Introduction

The study of Fe-rich nanocrystalline materials has a twofold interest. Firstly, they exhibit excellent soft magnetic properties as well as a high saturation magnetization, which make them interesting from the applications point of view [1, 2]. In addition, these materials are composed of two magnetic phases, amorphous and crystalline, which fluctuate spatially with a correlation length of nanometres and present complex magnetic interactions between them.

In order to account for the soft magnetic properties exhibited at ambient temperature by nanocrystalline FeSiBNbCu alloys, annealed under appropiate conditions [3], Herzer has previously considered the random anisotropy model [4]. Since the magnetically softest samples presented a high degree of crystallization (the crystalline volume fraction, x, was around 0.75) their crystalline anisotropy was successfully derived by considering them as single phase crystalline materials presenting an average grain diameter of the order of 10 nanometres. However, other experimental results provided evidence for the two-phase character of these ferromagnets, for instance, the increase of the coercive field occurring at the beginning of the crystallization process [5, 6], as well as at temperatures close to the Curie temperature of the amorphous phase [3, 7, 8]. In order to account with these phenomena several authors have optimiced the random anisotropy model on including the magnetic characteristics of the amorphous phase [7, 9–12].

In a previous work of some of the present authors, a new model that provides a qualitative explanation of the above-mentioned results has been proposed [12]. According to this picture, the effective magnetocrystalline anisotropy, k^{eff}, mainly depends on the exchange coupling

0953-8984/00/143255+11$30.00

between the crystallites that takes place through the amorphous matrix. This coupling is introduced by means of an effective exchange constant, A_{eff}, that depends on the ratio between the exchange correlation length of the pure amorphous phase, L_2, and the mean intergranular distance, D, given by

$$D = d_1[(\alpha/x)^{1/3} - 1] \tag{1}$$

where x is the crystalline volume fraction, d_1 is the average grain diameter and α is a geometrical factor that depends on the shape and the arrangement of the crystallites. If we consider a simple cubic (sc) arrangement of cubic crystallites, then $\alpha = 1$, and the crystallites only come into contact if the sample is fully crystallized ($x = 1$). Whereas, for spherical crystallites arranged in a sc or a face centred cubic (fcc) lattice, $\alpha = \pi/6$ or $\alpha = 2^{1/2}\pi/6$, respectively, and the particles are in contact for $x < 1$ [13].

For $D > L_2$ the exchange interaction coming from one crystallite does not reach the surface of the others and, hence, $A_{\text{eff}} = 0$. However, if the condition $L_2 > D$ is fulfilled, the crystallites are effectively coupled provided that the exchange interaction between them is strong enough to overcome the crystalline anisotropy. In this case, according to random anisotropy considerations, the effective anisotropy constant can be written as

$$k^{\text{eff}} = xk_1/N^{1/2} = x^2k_1^4d_1^6/A_{\text{eff}}^3 \tag{2}$$

where k_1 is the anisotropy constant of the crystalline phase and $N = xL^3/d_1^3$ is the number of crystallites within the exchange correlation length of the two-phase system, L.

If the crystallites are exchange decoupled, we can consider then as non-interacting single domain particles and the effective anisotropy is given by

$$k^{\text{eff}} = xk_1 + (1 - x)k_2 \tag{3}$$

k_2 being the anisotropy constant of the amorphous phase. In this case $N < 1$, or as deduced from (2), $d_1 > x^{-1/6}(A_{\text{eff}}/k_1)^{1/2}$. As can be noticed, the contribution of the amorphous phase to the effective anisotropy has not been neglected, as these conditions occur for low values of x. This is the case of Fe-rich nanocrystals at the beginning of the crystallization process or at temperatures close to the Curie temperature of the amorphous phase, T_{C2}.

The coercivity of a ferromagnetic material is proportional to k^{eff} through the following relation

$$H_c = pk^{\text{eff}}/\mu_0 M_S \tag{4}$$

M_S being the spontaneous magnetization, and p a dimensionless factor, close to unity, which depends on the particular type of magnetization process. Concerning the thermal dependence of H_c, in a single phase material composed either of coupled or decoupled grains, k^{eff} decreases with T faster than M_S. Hence, the coercivity decreases as T increases. However, in a two-phase system of coupled grains with $T_{C2} < T_{C1}$ (where T_{C1} is the Curie temperature of the crystalline phase) and $L_2 > D$, as the exchange interaction between crystallites occurs through the amorphous matrix, the effective exchange constant, A_{eff}, decreases with temperature faster than k_1 for $T < T_{C2}$, and as inferred from (2) and (4), H_c can increase with T [7, 10]. Furthermore, when A_{eff} falls below $x^{1/3}k_1d_1^2$ the system becomes decoupled.

In the present paper we relate the structural and magnetic features of FeZr-based nanocrystalline alloys using the above-mentioned model. The conditions giving rise to a decoupled structure at the beginning of the crystallization process are qualitatively explained.

2. Experiment

Amorphous ribbons with the nominal composition $Fe_{87.2}Zr_{7.4}B_{4.3}Cu_{1.1}$ (at.%) were obtained by the melt-spinning technique. In order to achieve different stages of the nanocrystallization

process, the samples were annealed under high vacuum for 1 h, at temperatures ranging from 713 K to 923 K.

The coercive field H_c was measured in an earth field compensated Förster coercimeter using samples of dimensions 20 μm $\times$ 3 $\times$ 10^{-3} m $\times$ 6 $\times$ 10^{-2} m; the magnetic field was applied along the ribbon axis. The temperature could be changed between 50 K and 300 K by means of an He flow cryostat. The state of crystallization in the samples was determined by x-ray diffraction (XRD) using Cu Kα radiation, the scan step was $2\theta = 0.02^\circ$ and the averaging time between steps was 10 s. The thermal evolution of the saturation magnetization was measured in a vibrating sample magnetometer at temperatures up to 1000 K and under an applied field of 80 kA m^{-1}.

The magnetic domain patterns of some selected samples were observed by the magneto-optical Kerr effect. In order to enhance the magnetic contrast, the samples were polished and covered with a ZnS antireflection coating before the thermal treatment.

3. Results and discussion

The evolution of the diffraction patterns with the annealing temperature, T_a, is plotted in figure 1. The pattern of the as-cast sample consists of an amorphous halo and no crystalline peaks can be resolved, whereas in the sample annealed at 713 K a weak maximum corresponding to the (110) reflection of α-Fe appears superimposed on the halo. After further annealing at higher temperatures the (200), (211) and (220) reflections can also be appreciated, and their intensity increases gradually with T_a. The presence of intermetallic compounds was not detected in any of the samples investigated.

The average grain diameter of the crystalline phase, d_1, was estimated from the full width at half maximum (FWHM) of the (110) α-Fe peak (corresponding to $2\theta \sim 45^\circ$) using the

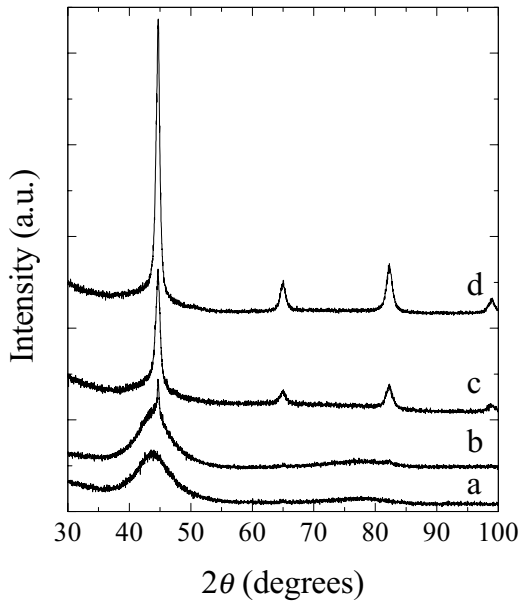

Figure 1. X-ray diffraction patterns of an as-cast sample (a) and annealed samples for 1 h at 713 K (b), 748 K (c) and 813 K (d).

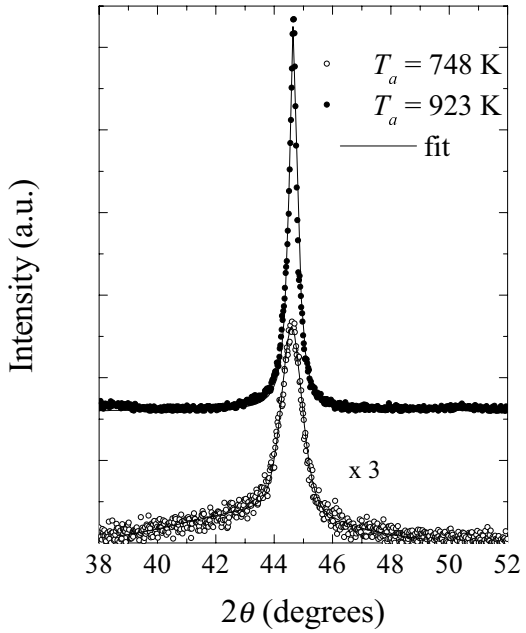

Figure 2. Diffraction peak profiles for the samples annealed at 748 K and 923 K (dots). The lines represent the fitted curves.

Table 1. Average grain diameter, d_1, crystalline fraction, x, saturation magnetization at room temperature $\mu_0 M_{300}$ and Curie temperature of the amorphous phase T_{C2}, versus annealing temperature, T_a. Uncertainties for the last significant figure are given in brackets.

T_a (K)	d_1 (nm)	x	T_{C2} (K)	$\mu_0 M_{300}$ (T)
As cast	—	0.007(1)	320	0.48(1)
713	—	0.015(1)	310	0.45(1)
748	10(1)	0.16(1)	335	0.79(2)
783	13(1)	0.42(1)	430	1.07(3)
813	13(1)	0.61(2)	450	1.34(4)
883	16(2)	0.71(2)	—	1.47(4)
923	25(4)	0.73(2)	—	1.50(4)

Scherrer equation. Previously, the diffraction spectrum was fitted to the sum of a Gaussian function, ascribed to the contribution from the amorphous phase, and a pseudo-Voigt function, corresponding to the crystalline phase (for details see [14]). For annealing temperatures over 813 K, the amorphous contribution vanishes and the diffraction spectra could be fitted to a single pseudo-Voigt function. As an example, Figure 2 shows both the experimental data and the fitting for the samples annealed at 748 K and 923 K. The d_1 values so obtained are shown in table 1: as can be seen, the average grain diameter is 10 nm for the sample annealed at 748 K, increases up to 13 nm for $T_a = 783$ K and remains constant for T_a below 883 K. For higher annealing temperatures d_1 increases up to 25 nm. In a recently published work [13], a similar increase of the average grain size with T_a has been reported in $Fe_{87}Zr_6B_6Cu$ ribbons.

Figure 3 shows the thermal dependence of the magnetization of some selected samples measured with an applied field of 80 kA m^{-1}. The $M(T)$ curves of the samples as cast

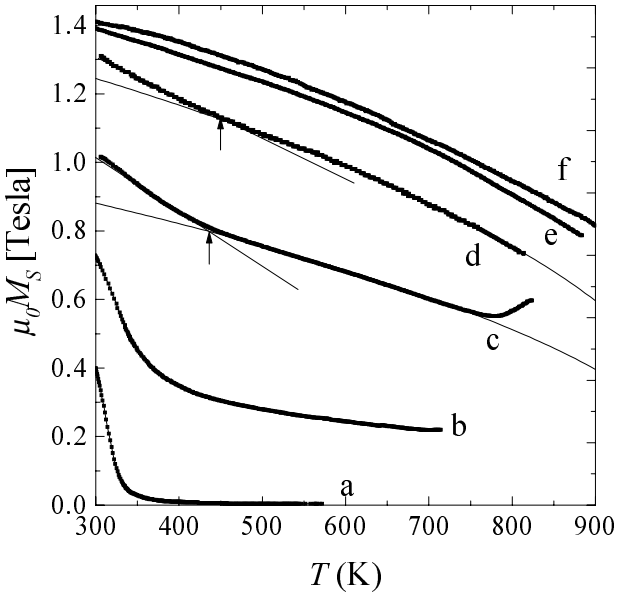

Figure 3. Thermal dependence of the magnetization, M, of the sample in the as-cast state (a) and annealed for 1 h at 748 K (b), 783 K (c), 813 K (d), 883 K (e) and 923 K (f).

and annealed at 713 K exhibit a single Curie temperature around 320 K, corresponding to the amorphous phase. Nevertheless, the $M(H)$ curves measured at $T = 523$ K (below the crystallization temperature) show hysteretic behaviour, which is attributed to the presence of some α-Fe particles (non-detectable by XRD in the as-cast sample). In this case, the crystalline fraction was estimated from the saturation magnetization at $T = 523$ K, after subtracting the paramagnetic contribution. In the samples annealed above 748 K, the $M(T)$ curves exhibit a higher Curie temperature which corresponds to α-Fe. In these samples, the crystalline fraction can be obtained by fitting the thermal dependence of the magnetization for $T > T_{C2}$, to the expression $M = xM_1(1 - T/T_{C1})^{0.36}$, where M_1 and T_{C1} are the saturation magnetization and the Curie temperature of the crystalline phase [3, 15]. The latter was assumed to be pure α-Fe, disregarding the effect due to the presence of solute elements [2]. Table 1 also shows the saturation magnetization measured at $T = 300$ K, M_{300}, and the Curie temperature of the amorphous phase, T_{C2}. For $T_a < 783$ K, T_{C2} could be obtained from the minimum of the $\mathrm{d}M/\mathrm{d}T$–T curves. However, in the samples annealed at 783 K and 813 K, the amorphous phase presents a wide distribution of Curie temperatures due to the penetration of the exchange field from the crystalline phase [8, 13]. Therefore, for $T_a \geqslant 783$ K, a maximum T_{C2} was estimated by determining the intersection point of the magnetization curve of the crystallites (extrapolated down to temperatures $T < T_{C2}$) and the contribution from the amorphous phase, fitted to a linear law. This value of T_{C2} has been considered to be representative, since the exchange decoupling between crystallites occurs above the maximum Curie temperature of the distribution (see [13]). The T_{C2} corresponding to the samples annealed above 813 K could not be estimated due to the weak contribution of the amorphous phase to the $M(T)$ curve. The D values calculated assuming different geometry are shown in table 2. When the crystallites are considered to be spherical, they come into contact for $T_a \geqslant 813$ K, if we suppose an sc array, or for $T_a \geqslant 923$ K, assuming an fcc arrangement (in the later case, the crystallites are

Table 2. Mean intergranular distance, D, derived through expression (1), for different crystallite shapes and arrangements: cubic crystals arranged in a single cubic (sc) mesh and spherical crystals arranged in an sc or a face centred cubic (fcc) mesh. Uncertainties for the last significant figure are given in brackets.

	D (nm)		
T_a (K)	cubes sc order	spheres sc order	spheres fcc order
As cast	—	—	—
713	—	—	—
748	9(1)	5.1(6)	7.0(7)
783	4.3(3)	1.0(1)	2.7(2)
813	2.3(2)	0.0(1)	0.87(8)
883	2.0(2)	0.0(2)	0.22(3)
923	2.8(4)	0.0(4)	0.12(3)

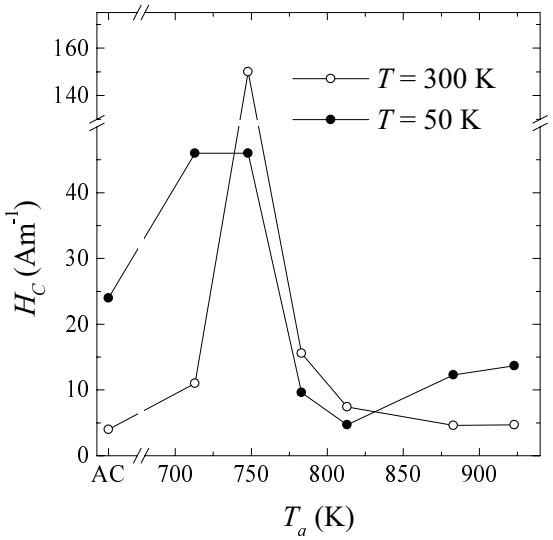

Figure 4. Evolution of the coercive field, H_c, with the annealing temperature, T_a, measured at $T = 300$ K and $T = 50$ K.

considered to be in contact, as the average intergranular distance is lower than the B covalent diameter, 0.164 nm).

Figure 4 shows the dependence of H_c on T_a measured at $T = 300$ K. As can be seen, the sample annealed at $T_a = 748$ K undergoes a large magnetic hardening comparing to the as prepared material. This increase of H_c at the beginning of the crystallization process has been previously reported in nanocrystalline $Fe_{73.5}Si_{13.5}B_9Nb_3Cu_1$ and $Fe_{87.2}Zr_{7.4}B_{4.3}Cu_{1.1}$ [5, 6], and was attributed to the existence of non-coupled crystallites.

For annealing temperatures above 748 K, the volume fraction of the α-Fe phase increases and the crystallites become coupled. As a consequence, the coercive field decreases to a low value similar to the as-cast state. As is clearly seen in equation (2) the effective anisotropy should increase with the average grain diameter and the crystalline fraction. However, the coercivity measured at room temperature remains almost constant with T_a for $T_a > 813$ K,

while d_1 and x grow. For the reasons listed below, an increase of the crystalline fraction on increasing annealing temperature can lead to a magnetic softening that counterbalances the effect of the grain enlargement: (i) The Curie temperature of the amorphous phase increases with the crystalline fraction (see table 1 and [13]). Accordingly, the effective coupling constant increases with T_a and, as can be derived from (2), this contributes to a reduction in k^{eff}. As a consequence, when the temperature is reduced to 50 K, well below T_{C2}, the coercive field increases monotonically with T_a (see figure 4). (ii) The saturation magnetization grows with x, leading to a reduction of H_c, see equation (4). (iii) As the saturation magnetostriction of the amorphous and crystalline phases present opposite signs [3], the average saturation magnetostriction decreases with the crystalline fraction [16, 17], leading to a diminution of the magnetoelastic anisotropy and, hence, of the coercive field.

However, in the samples annealed at 883 K and 923 K, these criteria cannot be applied as they present similar values of the crystalline fraction, and their grain diameters are very different. It must be stated that this behaviour has been already reported in $Fe_{88}Zr_7B_4Cu$ annealed at temperatures ranging from 873 K to 923 K [18]. According to the results shown in table 2, if we assume that the crystallites are arranged in an fcc lattice, the grains are in contact for $T_a = 923$ K. Consequently, an enhancement of the exchange coupling would be expected for this annealing temperature. However, assuming an sc arrangement, our model would fail to explain the magnetic softness of this sample. In this case, this discrepancy could be ascribed to changes in the crystalline fraction composition, or to an enhanced crystalline growth on the ribbon surface in the sample annealed at 923 K: as the x-ray measurements are sensitive to a thin layer below the sample surface (around 4 μm thick for $2\theta = 45^\circ$ [14]), a preferential surface growth could lead to the measurement of a grain diameter larger than that of the bulk. In order to elucidate these points, a more accurate structural characterization, perhaps using Mössbauer spectroscopy or transmission electron microscopy, is addressed.

With the aim of obtaining complementary information about the magnetic order, the domain patterns in the remanence state were observed at room temperature by magneto-optical Kerr effect. The images obtained in the samples as cast and annealed at 748 K and 883 K are shown in figure 5: the amorphous sample presents wide curved domains separated by 180° walls as well as narrow stress patterns. It is generally accepted that such domain patterns are originated by tensile and compressive stresses, respectively, induced by the rapid quenching process [19, 20]. The sample annealed at 883 K also shows regular and wide domain patterns, with the magnetization lying along the applied field direction. In both samples the magnetization reversal takes place by domain wall movement. However, the sample annealed at 748 K shows an irregular domain pattern similar to that observed in nanocrystalline FeSiBNbCu alloys at temperatures close to T_{C2} [21]. Therefore, this pattern also suggests the interruption of the exchange coupling between the crystallites.

In the sample annealed at 748 K, the estimated distance between crystallites is lower than $D = 9$ nm. As the typical value of L_2 at $T = 300$ K is of the order of 500 nm [6], $L_2 > D$. Nevertheless, the grains are exchange decoupled, as evidenced by the high value of the coercive field and the domain images. In [6] the condition $L_2 < D$ was assumed for this sample, supposing that a high value of the internal stresses reduced drastically the magnitude of L_2. However, since the measuring temperature is close to $T_{C2} = 335$ K, the decoupling can be attributed to the weakening of the exchange interaction (i.e. $d_1 > x^{-1/6}(A_{\text{eff}}/k_1)^{1/2}$). This picture is reinforced by the thermal dependence of the coercivity, shown in figure 6. As can be appreciated, for temperatures below 200 K the coercive field decreases indicating that the crystallites become coupled. As L_2 decreases on cooling, whereas A_{eff} increases, the decoupling character at $T = 300$ K is not due to the condition $L_2 < D$ but to $A_{\text{eff}} < x^{1/3}d_1^2k_1$. That is, at $T = 300$ K the exchange interaction coming from a crystallite reaches the others, but

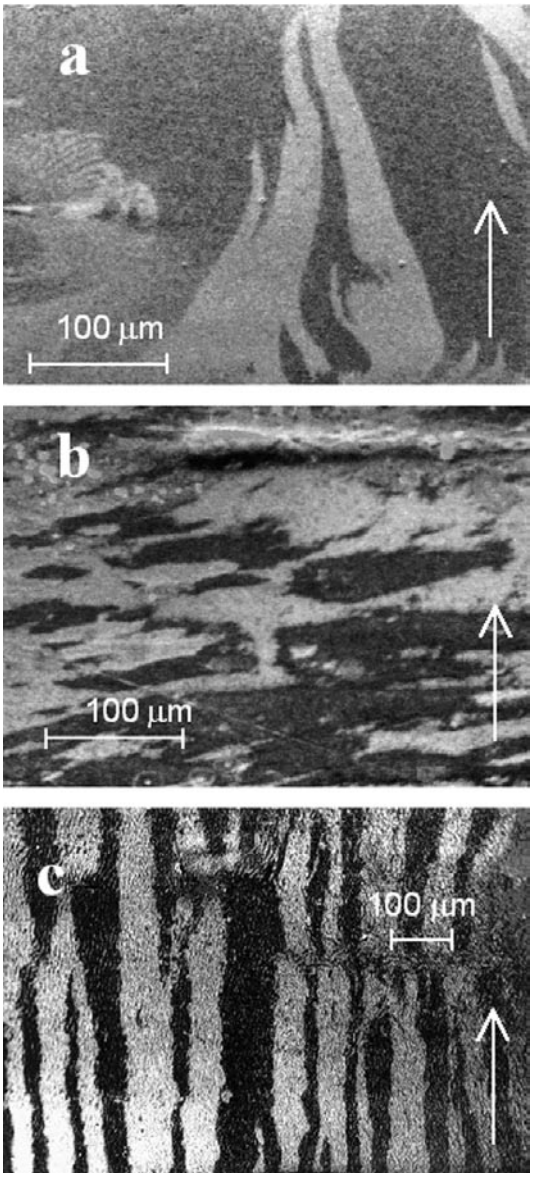

Figure 5. Domain patterns observed in the remanence state on the as-cast sample (a) and on the samples annealed for 1 h at 748 K (b) and 883 K (c). The arrow shows the direction of the applied field as well as the long axis of the ribbon shaped sample.

due to the proximity of T_{C2}, it cannot overcome the anisotropy energy. Furthermore, since N decreases for $T = 300$ K, L diminishes, being comparable to d_1, and therefore the crystallites act as pinning centres for the domain wall movement, as demonstrated in figure 5.

The temperature dependence of H_c shown in figure 6 can be elucidated by means of the described model. The samples as cast and annealed at $T_a = 713$ K and $T_a = 748$ K present a large volume fraction of amorphous phase. Therefore, the diminution of the coercive field at low temperature is due to the contribution of this phase, which anisotropy decreases with

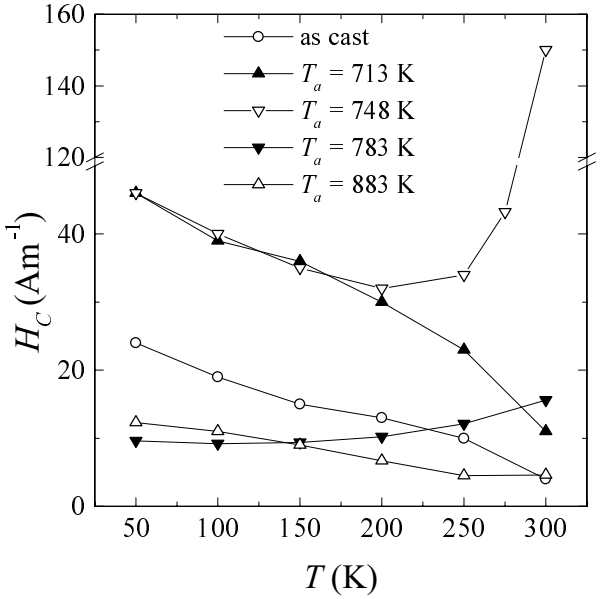

Figure 6. Thermal dependence of coercivity in the samples as cast and annealed at 713 K, 748 K, 783 K and 883 K.

T as a power of the saturation magnetization of the amorphous phase, M_2. As will be seen below, we can consider that the small amount of crystallites present in the samples as cast and annealed at 713 K is decoupled. In these samples the average grain diameter cannot be estimated from the diffraction data. However, as their crystalline fraction is lower than in the sample annealed at 748 K, we can reasonably suppose that the distance between crystallites is larger. Besides, these samples also show a lower T_{C2} than the sample annealed at 748 K, and thus they present a lower exchange constant. These two reasons lead us to suppose that the exchange interaction between crystallites in these samples is lower than in the sample annealed at 748 K. Moreover, the sample annealed at 713 K shows larger coercive field than the as-cast sample in the measuring temperature range, this points out the presence of a larger amount of uncoupled crystallites.

It is worth noticing that the samples annealed at 748 K and 713 K exhibit roughly the same coercivity for $T < 200$ K. Let us consider that $k_{748}^{\mathrm{eff}}(T)$ and $k_{713}^{\mathrm{eff}}(T)$ are the effective anisotropy constants of the samples annealed at 748 K and 713 K, respectively. If we disregard the differences in M_s and p between the two samples (see expression (4)), the value of k_{748}^{eff} should be similar to k_{713}^{eff} for $T < 200$ K. According to the previous description, in the sample annealed at 713 K the grains are exchange decoupled in the measured temperature range. Hence, $k_{713}^{\mathrm{eff}} = x'k_1$ for $T < 300$ K, where $x' = 0.015$ is the crystalline fraction of this sample. On the other hand, in the sample annealed at 748 K the crystallites are exchange coupled below 200 K and become decoupled at higher temperature. Accordingly, the anisotropy of this sample is given by $k_{748}^{\mathrm{eff}} = xk_1/N^{1/2}$ for $T < 200$ K and approaches to $k_{748}^{\mathrm{eff}} = xk_1$, where $x \approx 0.15$ (see table 1) as the temperature increases above 250 K. Therefore, for $T < 200$ K the condition $k_{748}^{\mathrm{eff}} \sim k_{713}^{\mathrm{eff}}$ occurs if $N \sim (x/x')^2 = 100$, i.e. if $L = (N/x)^{1/3}d_1 \sim 90$ nm, which is a reasonable value for the exchange–correlation length. As can be noticed, we have not considered the contribution of the amorphous phase for comparing the thermal evolution of k_{748}^{eff} and k_{713}^{eff}, since we can assume that is roughly the same in both samples.

The coercivity of the sample annealed at 783 K increases slowly on heating, due to the diminution of A_{eff}. In this sample $T_{C2} = 430$ K, is higher than that of the sample annealed at 748 K and the system remains coupled in the measuring temperature range. As a consequence, this sample is softer than the sample annealed at 748 K in the whole temperature range, even though it presents a larger crystalline fraction. The existence of a broad distribution of Curie temperatures leads to a slow thermal decrease of the exchange coupling, and, therefore, to a slow increase of the coercive field. Finally, in the sample annealed at 883 K, the contribution of the amorphous phase cannot be appreciated in the $M(T)$ curve (see figure 2). However, the slight increase of H_c measured from 250 K to 300 K indicates the presence of an intergranular phase with lower Curie temperature than the crystalline ones.

4. Conclusions

The effect of the structure on the coercive field and its thermal dependence, as well as on the domain structure, are qualitatively elucidated in nanocrystalline FeZrBCu by means of a previously proposed model that accounts for the effective anisotropy in two-phase nanocrystalline materials. According to this model, the low temperature thermal evolution of the coercivity is dominated by the exchange coupling between crystallites, which mainly depends on the Curie temperature of the amorphous phase.

The sample annealed at 748 K shows a large enhancement of the coercive field at room temperature. The thermal dependence of the coercivity evidences that this magnetic hardening is promoted by the weakening of the exchange interaction due to the proximity of the Curie temperature of the amorphous phase, T_{C2}. For annealing temperatures above 748 K the room temperature coercive field remains almost constant, even though the average grain diameter increases; this fact can be ascribed to the augmentation of the exchange coupling with x, due to the enhancement of T_{C2}.

Acknowledgments

This work has been performed within the framework of Acciones Integradas between Germany and Spain. The authors thank Ms T Dragon for the Kerr effect images.

References

[1] Yoshizawa Y, Oguma S and Yamauchi K 1998 *J. Appl. Phys.* **64** 6044
[2] Suzuki K, Makino A, Kataoka N, Inoue A and Masumoto T 1991 *Mater. Trans. JIM* **32** 93
[3] Herzer G 1989 *IEEE Trans. Magn.* **25** 3327
[4] Alben R, Becker J J and Chi M C 1988 *J. Appl. Phys.* **64** 6044
[5] Vázquez M, Marín P, Davies H A and Olofinjana A O 1994 *Appl. Phys. Lett.* **64** 3184
[6] Gómez-Polo C, Holzer D, Multigner M, Navarro E, Agudo P, Hernando A, Vázquez M, Sassik H and Grössinger R 1996 *Phys. Rev.* B **53** 3392
[7] Herzer G 1995 *Scr. Metall. Mater.* **33** 1741
[8] Hernando A and Kulik T 1994 *Phys. Rev.* B **49** 7064
[9] Hernando A, Vázquez M, Kulik T and Prados C 1995 *Phys. Rev.* B **51** 3581
[10] Hernando A, Marín P, Vázquez M, Barandiarán J M and Herzer G 1998 *Phys. Rev.* B **58** 366
[11] Suzuki K and Cadogan J M 1998 *Phys. Rev.* B **58** 2730
[12] Arcas J, Hernando A, Barandiarán J M, Prados C, Vázquez M, Marín P and Neuweiler A 1998 *Phys. Rev.* B **58** 5193
[13] Garitaonandia J S, Schmool D S and Barandiarán J M 1998 *Phys. Rev.* B **58** 12 147
[14] Knobel M, Santos D R, Torriani I L and Turtelli R S 1993 *Nanostruct. Mater.* **2** 339
[15] Slawska-Waniewska A, Gutowski M, Lachowicz H K, Kulik T and Matyja H 1992 *Phys. Rev.* B **46** 14 594

[16] Suzuki K, Makino A, Inoue A and Masumoto T 1991 *J. Appl. Phys.* **70** 6232
[17] Slawska-Waniewska A, Zuberek R and Nowicki P 1996 *J. Magn. Magn. Mater.* **157/158** 147
[18] Kim K S and Yu S C 1993 *IEEE Trans. Magn.* **29** 2679
[19] Vázquez M, Fernengel W and Kronmüller H 1983 *Phys. Status Solidi* a **80** 195
[20] Veider A, Badurek G, Grössinger R and Kronmüller H 1986 *J. Magn. Magn. Mater.* **60** 182
[21] Schäfer R, Hubert A and Herzer G 1991 *J. Appl. Phys.* **69** 5325